JOURNAL OF AGRICULTURAL AND FOOD CHEMISTRY

Article

pubs.acs.org/JAFC

Nutraceutically Inspired Pectin–$Mg(OH)_2$ Nanocomposites for Bioactive Packaging Applications

Francys K. V. Moreira,[†,§] Lais A. De Camargo,[†,⊗] José M. Marconcini,[†] and Luiz H. C. Mattoso*[,†]

[†]National Laboratory of Nanotechnology for Agribusiness (LNNA), Embrapa Instrumentation (CNPDIA), São Carlos (SP), Brazil.

[§]Postgraduate Program in Materials Science and Engineering (PPG-CEM), Federal University of São Carlos (UFSCar), São Carlos (SP), Brazil

[⊗]Department of Chemistry, Federal University of São Carlos (UFSCar), São Carlos (SP), Brazil

Supporting Information

ABSTRACT: This paper reports on the development of bioactive edible films based on pectin as a dietary matrix and magnesium hydroxide ($Mg(OH)_2$) nanoplates as a reinforcing filler. Nanocomposites of high-methoxyl (HM) and low-methoxyl (LM) pectins were prepared using the casting method at concentrations of $Mg(OH)_2$ ranging from 0.5 to 5 wt %. Atomic force microscopy and FTIR spectroscopy were employed to characterize the nanocomposite structure. The tensile properties and thermal stability of the nanocomposites were also examined to ascertain the effect of $Mg(OH)_2$ inclusion and degree of methoxylation. The results provided evidence that the $Mg(OH)_2$ nanoplates were uniformly dispersed and interacted strongly with the film matrix. The mechanical and thermal properties were significantly improved in the nanocomposite films compared to the control. $Mg(OH)_2$ nanoplates were more effective in improving properties of LM pectin. Preliminary migration studies using arugula leaves confirmed that pectin–$Mg(OH)_2$ nanocomposites can release magnesium hydroxide by contact, demonstrating their potential for magnesium supplementation in bioactive packaging.

KEYWORDS: *edible films, dietary fibers, magnesium hydroxide, fortificants, food packaging*

INTRODUCTION

Promoting consumer health is a current issue in the food industry in view of growing public awareness over the intake of healthier foods. In this context, developing new packaging systems capable of upgrading the nutritional value of foods has begun to receive special attention. Lopez-Rubio et al. coined the term "bioactive packaging" to refer to food packaging with a specific role in generating healthier foods.[1] These innovative technologies generally deal with functional ingredients, such as phytochemicals, vitamins, marine oils, and prebiotics, which can be directly included in the package or coating materials to enrich foods through migration.

Pectins are attractive biopolymers for creating bioactive packaging. They belong to the class of dietary fibers and serve as a functional, renewable, and nontoxic material. Some of the well-known health benefits of pectins include assisting weight loss and regulating gastrointestinal function, as well as protective and reversal effects against diabetes, cardiovascular diseases (CVD), and atherosclerosis.[2,3] Current evidence suggests that pectins also possess inhibitory action against the prometastatic protein galectin-3 (GAL3), thus playing a role in the prevention and reduction of carcinogenesis.[4]

Chemically speaking, pectins are a complex family of carbohydrates mainly composed of (1→4)-linked α-D-galacturonic acid (GalA). The GalA occurs as pure segment chains (homogalacturonan) and (1→2)-linked to α-L-rhamnose (Rha), to which side chains of complex glycans are attached (rhamnogalacturonans).[5,6] Various properties of pectins are influenced by the degree of methyl-esterification (DM) of the GalA units, apart from other fine molecular details. DM has been used to categorize pectins into two basic groups, namely, high-methoxyl (HM) pectins (DM > 50%) and low-methoxyl (LM) pectins (DM < 50%).[6]

Pectins are known for their excellent film-forming capacity; thus, they can be used to produce coatings or edible films with potential application in bioactive packaging. However, pectin-based films generally have poor moisture barrier, weak mechanical properties, and low thermal stability, requiring effective strategies to overcome these drawbacks.[7−9]

In recent years, nanotechnology concepts have been successfully applied to enhance the physical properties of coatings and edible films. Chitosan (CS) nanospheres remarkably improved mechanical strength and water vapor permeability of cellulose ether films.[10,11] Mechanical and water barrier properties of complex formulations involving guava purée were also improved due to the inclusion of CS nanospheres.[12] Other studies reported improvement in mechanical properties of edible films of mango purée,[13] chitosan,[14] and xylan-rich hemicellulose[15] with the addition of cellulose nanofibers. Hence, the inclusion of nanoreinforcements emerges as a suitable approach for enhancing the physical properties of pectin-based films. A basic aspect regarding this approach is that nanoreinforcements must also have food-grade properties because they will be part of an edible material.[16]

Received: March 4, 2013
Revised: June 21, 2013
Accepted: June 25, 2013
Published: June 25, 2013

Magnesium hydroxide ($Mg(OH)_2$) is an inorganic filler capable of meeting these requirements. It is a layered mineral used widely as an antacid in pharmacy, as a fertilizer, and as additive in the paper industry. Its crystalline structure comprises magnesium ions octahedrally coordinated by hydroxyl ions, forming electrically neutral layers stacked along the *c*-direction.[17] The hydroxyl ions characterize the surface of the layers, which have a thickness of 0.478 nm.[17,18] $Mg(OH)_2$ combines the advantages of being a reinforcing filler[19] and flame retardant[20,21] with the generally recognized as safe (GRAS, no. 1309-42-8) status, which means that it could potentially be used in edible films. Studies have reported that nanosized $Mg(OH)_2$ can impart better mechanical properties and thermal stability to packaging materials such as poly(ethylene terephthalate)[22] and polyethylene.[23] More recently, substantial improvements were also reported in the mechanical strength of starch films with the addition of plate-shaped $Mg(OH)_2$ with nanometric dimensions.[24]

$Mg(OH)_2$ is an interesting filler also due to the importance of Mg for health-related issues. Mg is the fourth most abundant cation in the human body, acting as an enzyme cofactor, and is essential to calcium homeostasis and neuromuscular functions.[25,26] Unfortunately, the estimated average requirement (EAR) of Mg (310−420 mg day^{-1}) is not satisfied by most diets in the world.[27,28] Clinical studies have associated magnesium deficiency (hypomagnesemia) with serious pathological disorders, such as osteoporosis, diabetes mellitus, congestive heart failure, and oxidative stress.[26−29] In this sense, the inclusion of $Mg(OH)_2$ into pectin bioactive films could also serve as an interesting approach for Mg supplementation, thus creating fortified edible materials for direct contact with foods.

The present study was aimed at developing nanocomposite films based on pectin and $Mg(OH)_2$ nanoparticles for use as bioactive packaging. In this first attempt, pectin−$Mg(OH)_2$ nanocomposite films were produced by the usual casting/evaporation method, and their mechanical and thermal parameters were measured to determine whether inclusion of $Mg(OH)_2$ nanoparticles enhances the properties of pectin matrices. Additionally, two different methoxylated pectins were used to examine the influence of DM on the properties of the nanocomposites. Migration contact tests were also carried out to gain first insight on the extra potential of pectin−$Mg(OH)_2$ nanocomposites for supplementing food products with magnesium.

MATERIALS AND METHODS

Materials. Low-methoxyl pectin (DM = 8.4%, M_w = 170,000 g mol^{-1}) and high-methoxyl pectin (DM = 74%, M_w = 130,000 g mol^{-1}) from peels of citrus fruits were purchased from CPKelco (Limeira, Brazil). Ammonium hydroxide (NH_4OH, 32 vol %), hydrochloride acid (HCl), and other reagents were used without further purification. Ultrapure water obtained by a purification system (Barnstead Nanopure Diamond, Thermo Fisher Scientific Inc., Dubuque, IA, USA) was used in all experimental procedures.

Pectin−$Mg(OH)_2$ Nanocomposite Preparation. $Mg(OH)_2$ nanoparticles were prepared by homogeneous precipitation at 25 °C as previously described.[24] To prepare the films, (LM or HM) pectin was dissolved in water at concentration of 1 wt % with a mixer operating at 12000 rpm. The pectin solution had its pH adjusted between 6 and 7 with a 0.2 mol L^{-1} NH_4OH solution to avoid the dissolution of $Mg(OH)_2$. Then, water volumes loaded with appropriate amounts of $Mg(OH)_2$ were added to the pectin solution to form mixtures with nanoparticle concentrations of 0.5, 1, 2.5, and 5.0 wt % (polymer mass basis). Subsequently, each mixture was homogenized by vigorous magnetic stirring for 1 h. Pectin−$Mg(OH)_2$ films were then produced by casting the mixtures on Teflon supports followed by water evaporation at 35 ± 2 °C in an oven. After complete drying, the films were detached from the supports and stored in plastic bags at room temperature prior to characterization procedures.

Scanning Electron Microscopy (SEM). Morphological characterization was performed using a Magellan 400 L microscope (FEI Co., Eindhoven, The Netherlands) running at 1−5 kV. The nanoparticle samples were deposited on conductive graphite paint (SPI Supplies, West Chester, PA, USA) prior to scanning. All images were generated using the secondary electron mode.

Atomic Force Microscopy (AFM). Surface morphology of films was examined by tapping-mode AFM (TM-AFM) on a Dimension V microscope (Veeco, Plainview, NY, USA). Height and phase images were simultaneously recorded side-by-side at a scan speed of 0.5 Hz employing cantilevers with nominal tip curvature radius of 10 nm and resonance frequency of 192.7 kHz. Computer analyses of raw data were performed using Gwyddion software, version 2.25.

FT-IR Vibrational Spectroscopy. FT-IR spectra were obtained with a spectrometer Spectrum 1000 (Perkin-Elmer, Boston, MA, USA) in the absorbance mode. Polymer films were directly analyzed after drying diluted bionanocomposite solutions on silicon plates. Powder samples were mulled in KBr disks (0.5 wt %). All spectra were collected with an accumulation of 32 scans at a resolution of 2.0 cm^{-1}.

Tensile Tests. Elastic modulus (E, GPa), tensile strength (σ_T, MPa), and elongation at break (ε_B, %) of the films were determined following the ASTM D882-09 standard.[30] The mechanical tests were performed on specimen strips (10 cm × 1 cm) using an EMIC DL3000 Universal Testing Machine (EMIC Equipamentos e Sistemas de Ensaio LTDA, Brazil) equipped with a 50 Kgf load cell. Samples were preconditioned at 24 ± 2 °C and 50 ± 3% relative humidity for at least 48 h prior to testing. A cross-head speed of 25 mm min^{-1} was used in these experiments. Five repetitions were performed for each film composition, and mean values were reported.

Thermogravimetric Analyses (TGA). Thermogravimetric (TG) and differential thermogravimetric (DTG) curves were obtained using a thermal analyzer Q500 (TA Instruments, New Castle, DE, USA). Samples (7−10 mg) were placed into Pt crucibles and heated from 25 to 600 °C at a rate of 10 °C min^{-1}. The measurements were performed under air condition (80% N_2 and 20% O_2) with a 60 mL min^{-1} flow. The following parameters were extracted from TG/DTG curves: water content (H_2O wt %), estimated as the mass loss at 150 °C; onset temperature at which polymer degradation starts (T_{onset}), which was assumed as a 3% mass loss after 150 °C; and temperature of maximum pectin decomposition rate (T_{max}). The analyses were repeated two times for each sample.

Migration Assay. The feasibility of pectin−$Mg(OH)_2$ nanocomposites to enrich food with Mg dosages was investigated using Rocket arugula (*Eruca sativa* Rocket) as a reference matrix. The contact assays were performed using the procedure reported by Avella et al.[31] with some modifications. Leaves of arugula weighing 1.0 g each were placed between two pieces of nanocomposite film and stored for 2.5 and 5 days in a chamber at 23 ± 2 °C and 50 ± 3% relative humidity. The films were then separated and leaves were freeze-dried under vacuum of 1.33 × 10^{-4} bar (Supermodulyo Freeze-Dryer, Thermo Fisher Scientific Inc., Kansas City, MO, USA). The dried leaf mass was registered, and the leaves were calcined in a muffle at 600 °C for 4 h. The obtained ashes were digested with 1.0 mL of 6.0 mol L^{-1} HCl solution in an oil bath at 130 °C and quantitatively transferred using a 0.25 mol L^{-1} HCl solution until a final volume of 25 mL. The concentrations of magnesium in solution were determined by flame atomic absorption spectrometry (FAAS) conducted on an AA240FS Varian spectrometer (Varian Inc., Palo Alto, CA, USA) (air/acetylene flame and 202.6 nm wavelength). Linear function (r^2 = 0.997) was obtained using several dilutions of Mg standard solution 1000 mg L^{-1} in a concentration range from 0 to 200 mg L^{-1}. All treatments were prepared in duplicate and the determination of magnesium was repeated three times. Mg contents in arugula leaves were expressed in 1 mg 100 g^{-1}.

Statistical Analyses. One-way analysis of variance (ANOVA) was applied to the data, and means were compared using Bonferroni's test at a confidence level of 95% ($p < 0.05$). All statistical calculi were done with the Origin software, version 6.0 (Origin Lab, Northampton, MA, USA).

RESULTS AND DISCUSSION

$Mg(OH)_2$ Nanoplates. $Mg(OH)_2$ nanoparticles have been synthesized by means of a facile route consisting of direct precipitation of Mg^{2+} ions in supersaturated alkaline medium.[24] Observations by SEM revealed that $Mg(OH)_2$ nanoparticles had a plate-like shape with irregular edges (Figure 1). The average diameter and thickness of the $Mg(OH)_2$ nanoplates previously measured were 80 ± 23 and 9 ± 2 nm, respectively.[24]

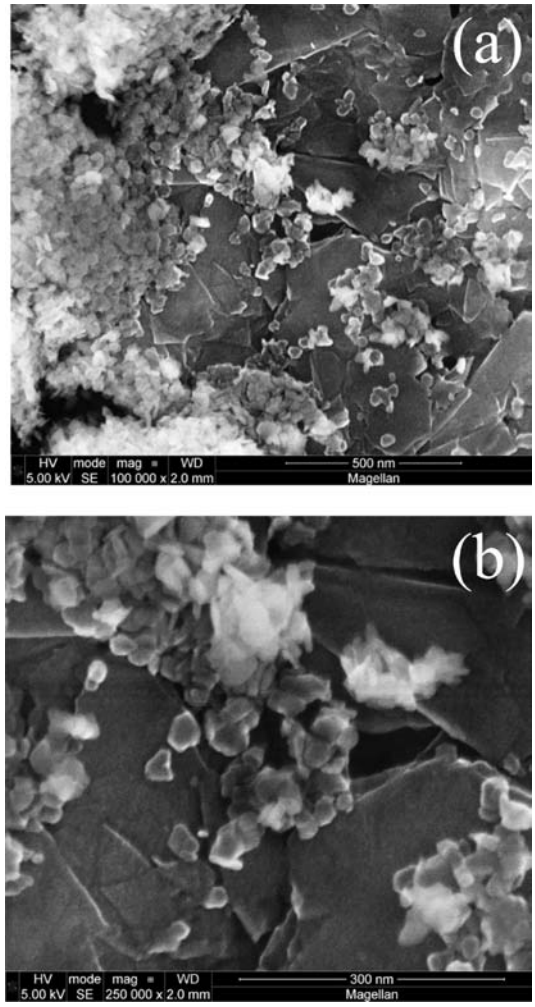

Figure 1. High-resolution SEM micrographs of $Mg(OH)_2$ nanoplates: (a) scale bar = 500 nm; (b) scale bar = 300 nm.

Structure of the Edible Nanocomposites. The pectin–$Mg(OH)_2$ edible films were flexible and transparent and had a bronze-like color. The films were also homogeneous, suggesting that $Mg(OH)_2$ and pectins were uniformly mixed. Nanocomposites with exfoliated or/and intercalated morphology cannot be formed from pectin and $Mg(OH)_2$. This is due to the interlamellae space of the $Mg(OH)_2$ structure (1.9 Å),[32] which is much short to allow penetration of polymer chains or even smaller molecules. Despite that, the dispersion state of the nanofiller in the polymer matrix is a key feature to elucidate once it correlates with the physical properties of the nanocomposites.

Height and phase imaging in TM-AFM was then employed to describe the resulting dispersion of the $Mg(OH)_2$ nanoplates in the pectic nanocomposites. Figure 2 displays TM-AFM images of the HM pectin and LM pectin edible films without nanoparticles. The nanocomposite film containing 5 wt % $Mg(OH)_2$ was chosen to compare morphologies and its images have also been included in Figure 2. Height images showed that all films had reasonably smooth surfaces. It was very difficult to identify the location of single $Mg(OH)_2$ nanoplates within the pectin matrices, even for the highest concentration; however, no morphological characteristic was found to evidence the formation of nanoparticle agglomerates. This was particularly supported by the phase images, where a homogeneous structure can be verified for all nanocomposites. These results suggest that $Mg(OH)_2$ nanoplates were well dispersed and enveloped by the pectin matrices.

The nanofiller dispersion observed in the nanocomposites can be discussed in terms of the characteristic surface charge of pectins and $Mg(OH)_2$ (Figure 3). Empirical observations by zeta-potential have shown that potentials of ±25–30 mV lead to a stable colloidal suspension due to sufficient amount of equal charges that promote repulsion between components.[33,34] In the present case, most of the carboxylic groups (pK_a ca. 3.5–4.0)[35,36] of pectins were deprotonated when the pH of the film-forming solution was increased to 6–7 (see Materials and Methods). Such pH values are sufficiently high to generate negative potentials in pectin solutions over a range from −30 to −60 mV.[35−37] Additionally, the pH of the film-forming solution imparted positive charges on the nanoplate surface because the point of zero charge (PZC) of $Mg(OH)_2$ is ca. 10–12.[38] Therefore, it is suggested that the good nanofiller dispersion reached in the pectin–$Mg(OH)_2$ nanocomposite films was due to the adsorption of negatively charged pectin chains on the positively charged surface of $Mg(OH)_2$ nanoplates, thus preventing their agglomeration. Nevertheless, it is necessary to account for the surface roughness parameters (R_{rms}) obtained from the height images (Table S1 in the Supporting Information). Studies have reported that an increase in surface roughness could relate to a poor dispersion of the nanofiller in the polymer matrix. For instance, Kaboorani et al. reported that agglomeration of nanocrystalline cellulose in poly(vinyl acetate) led to surface reorganization, increasing the surface roughness parameters of films.[39] As pointed out in Table S1 of the Supporting Information, R_{rms} values of pectin–$Mg(OH)_2$ nanocomposites were higher than those of the neat pectin films. This led to the conclusion that the dispersion of $Mg(OH)_2$ nanoplates in the pectin matrices was not very high, which in fact was expected.

FTIR Spectra. Infrared vibrational spectroscopy was applied to detect chemical interactions between the pectins and the $Mg(OH)_2$ nanoplates. Figure 4 shows the FT-IR spectra of neat components and their related nanocomposites containing 1 and 5 wt % $Mg(OH)_2$. Neat pectin film spectra exhibited typical vibration bands at 3370–3350 cm^{-1} related to stretching OH (ν_{OH}) of water molecules and hydroxyl groups of pectins. Stretching CH (ν_{CH}) vibrations of pyranoid rings were also observed at 2940 cm^{-1}. The characteristic strong band assigned to the stretching C=O vibration of carboxylic ($\nu_{(C=O)COOH}$) and ester ($\nu_{(C=O)COOR}$) groups was clear at ca. 1742 cm^{-1}. Furthermore, two additional vibration bands related to

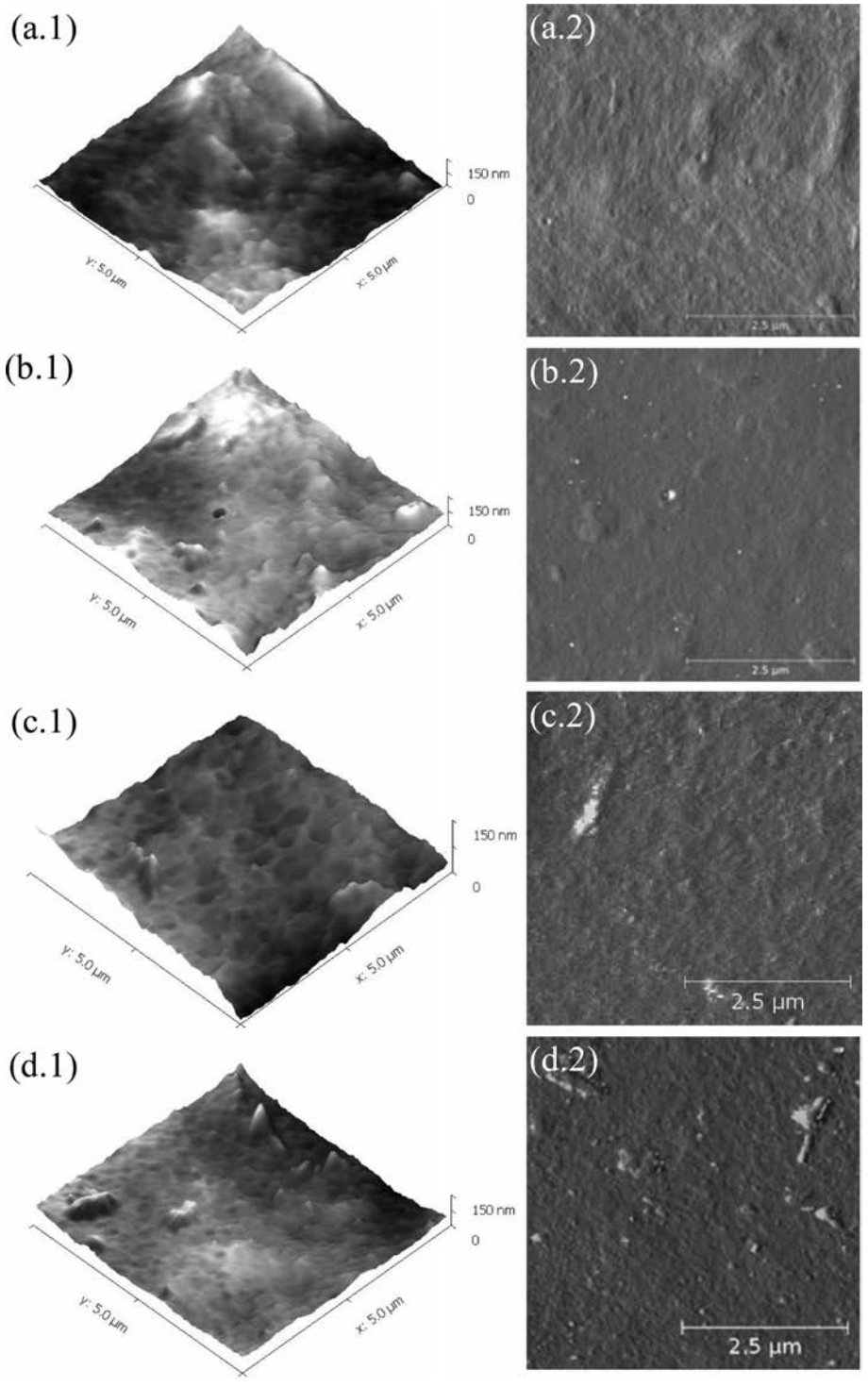

Figure 2. TM-AFM characterizations for (a) pure LM pectin film; (b) (LM pectin)−$Mg(OH)_2$ nanocomposite with 5 wt % $Mg(OH)_2$; (c) pure HM pectin film; (d) (HM pectin)−$Mg(OH)_2$ nanocomposite with 5 wt % $Mg(OH)_2$. The pictures on the left are 3D views from height images, and the pictures on the right are phase images. The scanning scale is 5 × 5 μm.

carboxylic groups in their carboxylate form were observed in the spectra of the neat biopolymer films: asymmetric stretching ($\nu_{(COO-)asym}$) at 1603 cm^{-1} and symmetric stretching ($\nu_{(COO-)sym}$) at 1439 cm^{-1}.[40] The spectral region below 1400 cm^{-1} encompasses the "fingerprint" region of polysaccharides, which contains highly complex overlapping of skeletal C−O and C−C vibration bands from glycosidic bonds and pyranoid rings.[40]

The $Mg(OH)_2$ spectrum exhibited typical vibration bands at 3697 cm^{-1} attributed to ν_{OH} in hydroxide layers and Mg−O stretch−bend motions at 576 and 448 cm^{-1}.[18,41] The bands at 3428 and 1603 cm^{-1} can be assigned to the ν_{OH} and δ_{H-O-H}, respectively, of water molecules coordinated to magnesium.[41] A last vibration band observed at 1429 cm^{-1} may be attributed to $\nu_{(C=O)asym}$ of carbonate, which was possibly formed by the reaction of $Mg(OH)_2$ with atmospheric CO_2 during synthesis.

dx.doi.org/10.1021/jf402110g | J. Agric. Food Chem. 2013, 61, 7110−7119

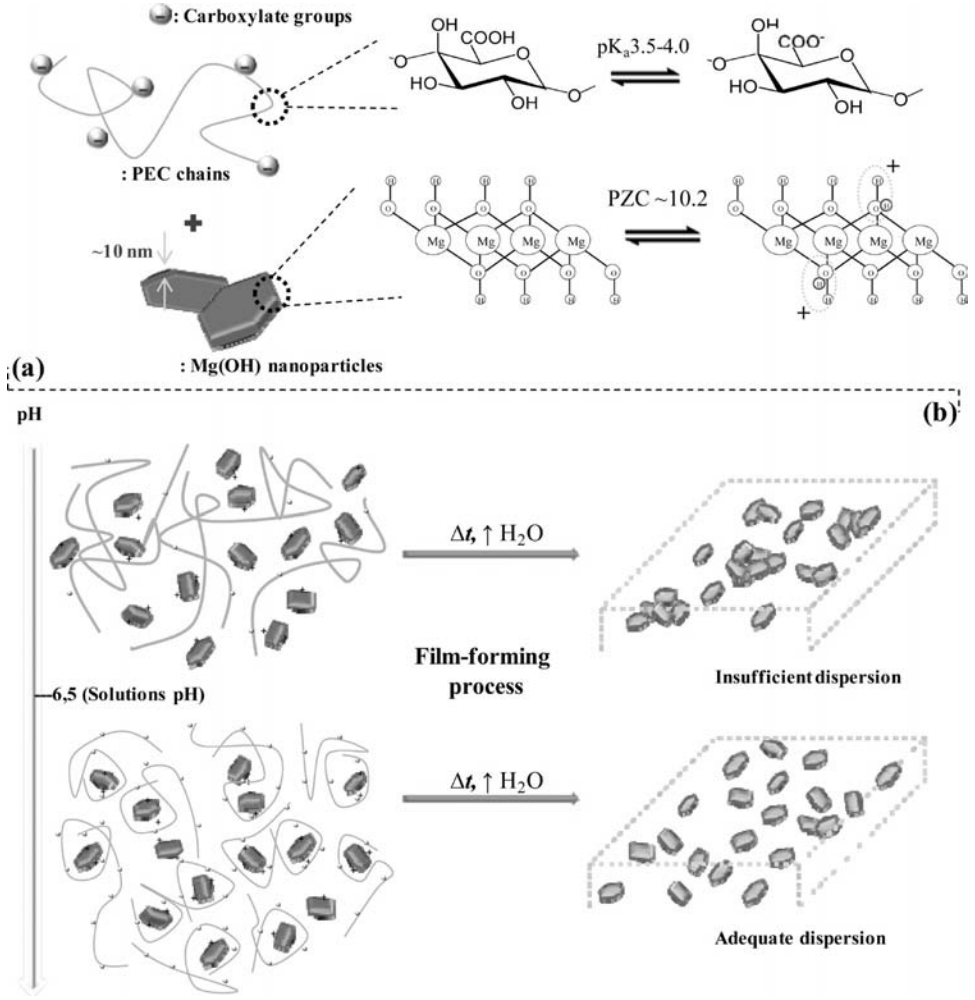

Figure 3. Schematic illustration of the pectin−$Mg(OH)_2$ nanocomposite films obtained by casting: (a) states of protonation of the pectin and $Mg(OH)_2$; (b) influence of the pH on the $Mg(OH)_2$ nanoplate dispersion and proposed structure for the nanocomposite films.

The FTIR spectra of nanocomposites showed changes in the vibration bands of pectin due to the presence of $Mg(OH)_2$ nanoplates. The $\nu_{(COO-)asym}$ band at 1603 cm^{-1} shifted to higher wavenumbers as the $Mg(OH)_2$ concentration was increased, whereas the $\nu_{(COO-)sym}$ band shifted to lower wavenumbers, which was also accompanied by a gradual decrease in the intensity of the $\nu_{(C=O)}$ band at 1741 cm^{-1}. These trends reveal a perturbation in the local environment of the carboxylic groups, providing strong evidence that there were chemical interactions between pectins and $Mg(OH)_2$ nanoplates. It was interesting to note that a discrepancy existed in the wavenumber shift ($\Delta\nu$) of the $\nu_{(COO-)sym}$ band regarding the DM of the pectins. Considering the neat films and nanocomposites containing 5 wt % $Mg(OH)_2$, the shift to lower wavenumbers, that is, lower energies, was greater for the LM pectin ($\Delta\nu$ = 16 cm^{-1}) than for the HM pectin ($\Delta\nu$ = 5 cm^{-1}). This difference may indicate stronger interactions between the LM pectin and the $Mg(OH)_2$ nanoplate surface due to the larger quantity of polar groups in this type of biopolymer.

The ν_{OH} bands of hydroxyl groups also appeared changed in the spectra of the nanocomposites. They were somewhat less intense in comparison to those in the spectra of neat films, suggesting that pectin and $Mg(OH)_2$ surface established interactions through hydrogen bonding. The existence of hydrogen bonds could be also deduced by inspecting the ν_{OH} band of $Mg(OH)_2$ layers; however, such a band was absent in the spectra of the nanocomposites. A possible reason for this is the displacement of this band toward lower wavenumbers, thus overlapping with the ν_{OH} band of pectin hydroxyl groups. Such a behavior is not uncommon as it was verified, for instance, in chitosan/sepiolite nanocomposites in which the formation of hydrogen bonds has been pointed out.[42] The bending vibrations of Mg−O bonds were not observed in the nanocomposite spectra, probably due to the easy interference of others compounds on these low-frequency bands[18] or, more likely, the low concentrations of $Mg(OH)_2$. Figure S1 in the Supporting Information displays additional spectra in the 1000−400 cm^{-1} range for nanocomposite films containing 7.5 and 10 wt % $Mg(OH)_2$. For both samples, the Mg−O vibration band is clearly detected at ~450 cm^{-1}, confirming the influence of the $Mg(OH)_2$ concentration on the FTIR measurements.

Chemical interactions between nanofiller and matrix are important features in nanocomposites, once they are directly correlated with the superior properties of these hybrids. Therefore, enhanced properties for the pectin−$Mg(OH)_2$ edible nanocomposites can be expected from the interactions revealed by FTIR, particularly for films based on low-methoxyl pectins.

dx.doi.org/10.1021/jf402110g | J. Agric. Food Chem. 2013, 61, 7110−7119

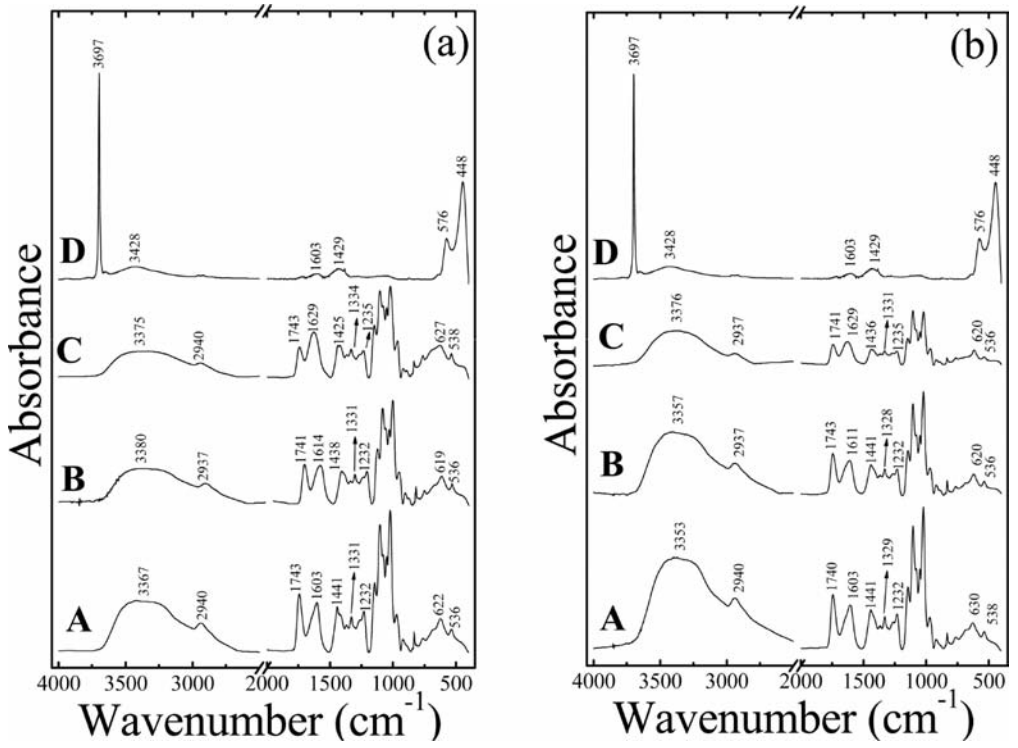

Figure 4. FTIR spectra collected in absorbance mode for (a) (LM pectin)−$Mg(OH)_2$ nanocomposites and (b) (HM pectin)−$Mg(OH)_2$ nanocomposites: (A) 0 wt % $Mg(OH)_2$; (B) 1 wt % $Mg(OH)_2$; (C) 5 wt % $Mg(OH)_2$; (D) neat $Mg(OH)_2$.

Table 1. Mechanical and Thermal Data of Pectin−$Mg(OH)_2$ Edible Nanocomposites[α]

MH (wt %)	E (GPa)	σ_T (MPa)	ε_B (%)	H_2O (%)	T_{onset} (°C)	T_{max} (°C)
			LM Pectin			
0.00	1.3 (0.1)a	44.8 (1.1)a	4.0 (0.2)a	13.3 (1.6)a	202.2 (0.1)a	225.9 (1.7)a
0.50	2.6 (0.1)b	53.7 (1.8)b	3.5 (0.4)ac	13.7 (2.1)a	203.7 (1.5)a	226.6 (1.9)ac
1.00	2.6 (0.1)b	55.8 (0.8)b	2.7 (0.2)bc	13.5 (1.7)a	201.2 (1.2)a	226.4 (3.2)a
2.50	2.7 (0.1)b	47.1 (0.8)a	2.4 (0.5)bc	14.9 (0.4)a	209.7 (0.7)b	235.4 (1.2)bcd
5.00	2.8 (0.1)b	63.3 (2.9)c	2.4 (0.2)b	15.9 (3.8)a	211.8 (2.0)b	240.4 (3.8)ad
			HM Pectin			
0.00	2.7 (0.1)a	40.1 (2.4)a	1.8 (0.2)a	13.3 (1.1)a	199.5 (2.7)a	226.4 (3.2)a
0.50	2.8 (0.1)a	54.2 (2.0)b	2.9 (0.3)b	13.5 (2.1)a	200.8 (2.5)a	225.9 (1.2)a
1.00	2.6 (0.2)a	56.4 (2.4)b	3.1 (0.4)b	13.5 (1.7)a	201.7 (5.1)ac	225.9 (4.2)ac
2.50	2.9 (0.2)a	44.7 (1.4)a	1.8 (0.2)a	15.0 (2.2)ab	210.8 (0.1)bc	234.3 (0.7)b
5.00	3.0 (0.1)a	44.3 (3.8)a	2.0 (0.2)a	17.0 (2.0)b	209.3 (1.1)a	239.6 (2.9)bc

[α]Mean value (standard error). Means in the same column bearing the same letter are not significantly different ($p > 0.05$).

Mechanical Properties. Elastic modulus (E), tensile strength (σ_T), and elongation at break (ε_B) of the pectin−$Mg(OH)_2$ edible nanocomposites are reported in Table 1. Changes in tensile properties can be noted due to the addition of $Mg(OH)_2$ nanoplates, suggesting that the nanoparticles modified the stress transfer within the pectin matrices. Table 1 also reports that different mechanical behavior for pectin−$Mg(OH)_2$ nanocomposites occurred regarding the DM of pectins. Earlier studies have reported that LM pectins are mechanically more resistant than HM pectins because of the greater number of polar groups that favor the cohesion between the chains through hydrogen bonding.[40,43] In the present case, LM pectin film had lower E than HM pectin film due to the high amount of carboxylate groups ($-COO^-$) in the former, thus reducing the interactions between chains through electrostatic repulsion.[36] On the other hand, the LM pectin film had a slightly greater σ_T, which can be directly associated with its greater weight-average molecular weight (M_w). The influence of DM on the mechanical properties of the pectin−$Mg(OH)_2$ nanocomposites was then expected on the basis of these previous findings.

In (LM pectin)-based nanocomposites, E and σ_T significantly increased by 100 and 33%, respectively, after the addition of 0.5 wt % $Mg(OH)_2$ ($p < 0.05$), whereas a slight decrease in ε_B occurred in comparison to neat LM pectin film ($p > 0.05$). With further increase in $Mg(OH)_2$ concentration, E and σ_T values continued to increase, although without significant differences ($p > 0.05$). However, the σ_T value of the nanocomposite containing 5 wt % $Mg(OH)_2$ was significantly greater than that of the other compositions ($p < 0.05$). Such behavior closely resembles that found in polymer nanocomposites with a homogeneous dispersion of the filler at nanoscale,[44,45] providing good evidence of the interfacial interactions between the LM pectin and $Mg(OH)_2$ nanoplates.

dx.doi.org/10.1021/jf402110g | J. Agric. Food Chem. 2013, 61, 7110−7119

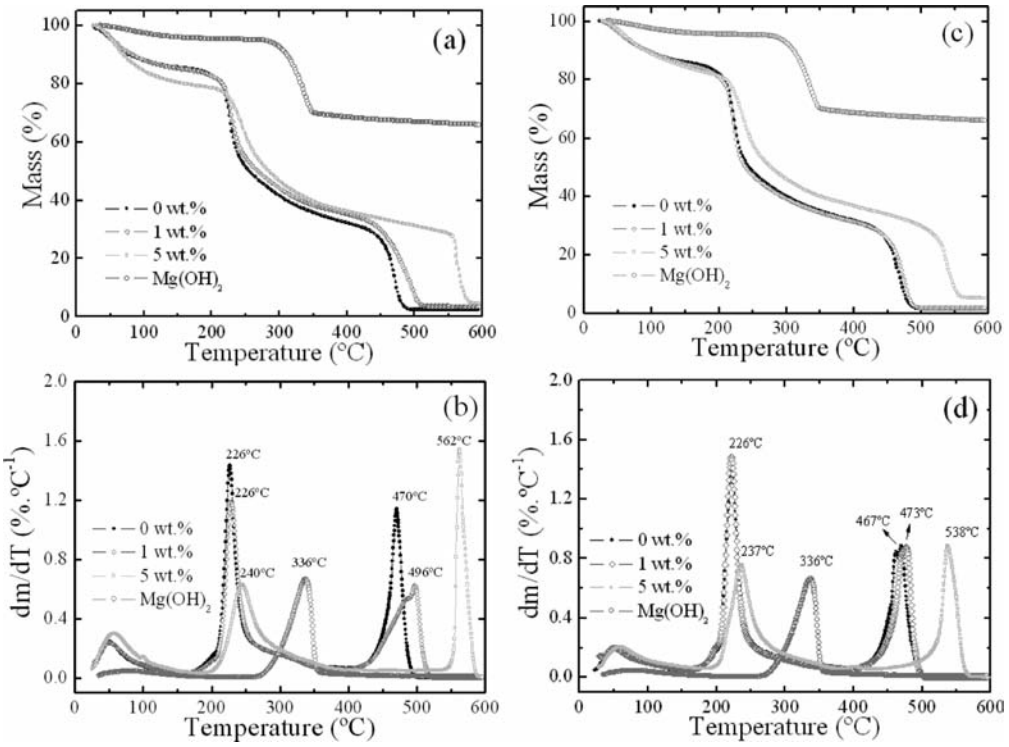

Figure 5. Thermogravimetric analysis curves (thermogravimetric, top; differential thermogravimetric, bottom) for the pectin–$Mg(OH)_2$ nanocomposites (a) and (b) LM pectin; (c) and (d) HM pectin. (Heating rate of 10 °C min^{-1} and synthetic air atmosphere with 60 mL min^{-1} flow.)

In support to this, ε_B values of nanocomposites decreased as $Mg(OH)_2$ concentration increased, differing from that of the neat matrix at 1 wt % ($p < 0.05$). The effective LM pectin–$Mg(OH)_2$ interactions probably constricted the flow of the pectin chains under load, thus reducing the elongation of the nanocomposites.

Different trends were observed for tensile properties of (HM pectin)–$Mg(OH)_2$ nanocomposite films. At low $Mg(OH)_2$ concentrations (0.5–1 wt %), σ_T and ε_B values were significantly greater than those of neat HM pectin film ($p < 0.05$), thus suggesting an enhanced mechanical performance of the HM pectin nanocomposites. This could also be related to homogeneous dispersion of the $Mg(OH)_2$ nanoplates in the matrix, as discussed above for the LM pectin nanocomposites. However, σ_T and ε_B decreased when the $Mg(OH)_2$ concentration was 2.5 wt % or higher, being statistically comparable to those of neat film ($p > 0.05$). This could indicate a lack of affinity between the $Mg(OH)_2$ nanoplates and HM pectin, in such a way that when large amounts of nanoparticles were used, the highly incompatible interfacial area formed in the nanocomposites led to an easier mechanical failure. Accordingly, it was observed that E of the (HM pectin)–$Mg(OH)_2$ nanocomposites increased slightly with $Mg(OH)_2$ concentration, but such variations were not sufficiently high to differ from that of neat film ($p > 0.05$). Probably, the large quantity of nonpolar methoxyl groups in HM pectin obstructed the chemical interactions with the $Mg(OH)_2$ nanoplates, and the stress transfer at the filler–matrix interface resulted in a narrow increase of tensile properties for such nanocomposites.

In summary, tensile tests showed that $Mg(OH)_2$ nanoplates were more effective in improving the mechanical properties of LM pectin edible films due to a larger number of polar groups accessible to interact with the hydroxyl groups of the hydroxide layer surface. These observations are in good agreement with the results obtained by FTIR.

Thermal Stability. Figure 5 displays TG and DTG curves of neat pectin films, neat $Mg(OH)_2$, and some of their nanocomposites. It is noticeable that the thermal behavior of the films, analogous for both pectins, was modified upon addition of $Mg(OH)_2$. In general, TG and DTG curves showed three mass loss stages: adsorbed water release (45–150 °C), decomposition of pectin chains (200–300 °C), and combustion of the polymeric residue ($T > 400$ °C).[7] With increasing $Mg(OH)_2$ concentration, DTG peaks related to pectin decomposition were shifted toward higher temperatures, revealing an increased thermal stability for the pectin–$Mg(OH)_2$ nanocomposites. The parameters from thermal analyses were collected for all prepared films and are also reported in Table 1.

The water content was in the range of 13–17 wt % for all films. The addition of $Mg(OH)_2$ nanoplates in concentrations up to 1 wt % resulted in small changes in the degradation temperatures of nanocomposites, originating T_{onset} and T_{max} values comparable to those of neat films ($p > 0.05$). As $Mg(OH)_2$ concentration increased from 2.5 wt %, on the other hand, there was a sharp increase in these parameters ($p < 0.05$). Cavallaro et al. reported similar trends in pectin-based films and different types of nanoclays. It was observed that the clay morphology played a role in the thermal stability of the nanocomposites, and their T_{max} values increased by 10 °C with the addition of fillers at levels of ca. 80 wt %.[9] Here, analogous increases were observed when much lower nanoparticle concentrations were added to the pectins. For example, T_{onset} and T_{max} increased by 10 and 15 °C, respectively, when the $Mg(OH)_2$ concentration was increased from 0 to 5 wt % ($p < 0.05$). Therefore, it is reasonable to assume that substantial

thermal stability improvements occurred for the pectin−$Mg(OH)_2$ nanocomposites, which originated from a strong ability of $Mg(OH)_2$ in hindering the decomposition of pectin.

It has been well described in the literature that the main flame retardant effect of $Mg(OH)_2$ is based on its endothermic decomposition, which produces water in a single step. This reaction withdraws heat from the surrounding medium of $Mg(OH)_2$, retarding the decomposition of the polymer matrix.[20,21] Nevertheless, such a mechanism is functional only when the decomposition temperatures of $Mg(OH)_2$ and polymer overlap. Hence, the endothermic dehydroxylation of $Mg(OH)_2$ cannot explain the increased thermal parameters of the edible nanocomposites because the decomposition steps of pectin and $Mg(OH)_2$ differ by almost 100 °C (Figure 4). TGA data suggest that other factors determined the thermal stability of these hybrids. Highly dispersed $Mg(OH)_2$ nanoplates probably acted as an insulating barrier against the transport of oxygen and decomposition gases.[7,44] This is consistent with the homogeneous structures of the nanocomposites revealed by TM-AFM. The presence of well-dispersed $Mg(OH)_2$ could also have reduced the thermal energy available to decompose the pectins, due to its greater heat capacity.[20] To support these propositions, an additional LM pectin film was produced by incorporating 3.45 mol of Mg^{2+} ions (Mg^{2+} molar quantity equal in nanocomposite with 5 wt % $Mg(OH)_2$), and its TG/DTG curves were collected (Figure S2 in the Supporting Information). No improved thermal stability was found in this sample; on the contrary, the decomposition of LM pectin was accelerated in the presence of free Mg^{2+} ions. This confirms that the better thermal stability of pectin−$Mg(OH)_2$ nanocomposites was a structural effect caused by the dispersion of the hydroxide nanoplates.

A last result seen in TGA is that the presence of $Mg(OH)_2$ nanoplates strongly affected the stability of the nanocomposites even after the pectin decomposition. This was clearly observed for the samples containing 5 wt % $Mg(OH)_2$ in which the third step had its T_{max} increased by ∼80 °C. Additional XRD characterizations of the calcined nanocomposite have shown an amorphous structure up to 350 °C and just occurrence of MgO as the final residue at 600 °C, meaning that no different compounds were formed than those expected from an independent pathway of thermal decomposition (Figure S3 in the Supporting Information). Such behavior suggests that $Mg(OH)_2$ nanoplates acted as an insulating barrier against the oxidation of the pectin residue and corroborates the structural effect proposed for the pectin−$Mg(OH)_2$ nanocomposites. Nevertheless, more studies will be necessary to describe accurately the mechanism involving the decomposition of these hybrids at high temperatures.

Migration of $Mg(OH)_2$. The pectin−$Mg(OH)_2$ nanocomposite films developed in this study were intended as bioactive materials principally due to the roles of pectin as dietary fiber. Moreover, the inclusion of $Mg(OH)_2$ renders these hybrids good fortifiers to foods, given the importance of Mg to human health. Initially, it was important to check this extra function of the pectin−$Mg(OH)_2$ nanocomposites by performing contact migration assays. As pectin films were highly unstable under moisture conditions (they solubilized in contact with water), a moderately dried food had to be used. Arugula was then chosen as the reference matrix due to its moderate water activity and smooth leaves, which improved the contact with films. Preliminary assays were carried out using nanocomposites with the highest nanoparticle concentration (5 wt %) to more easily detect a possible migration of $Mg(OH)_2$. The monitoring was done by the total quantity of Mg in arugula leaves. The results obtained for two different contact times are shown in Figure 6.

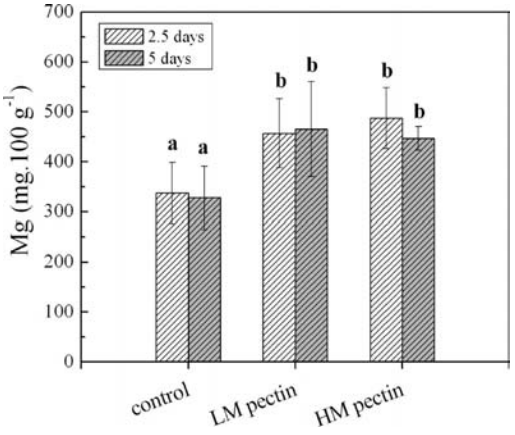

Figure 6. Total Mg contents (1 mg 100 g^{-1}) in arugula leaves determined by FAAS before (control) and after contact with pectin−$Mg(OH)_2$ nanocomposites (5 wt % $Mg(OH)_2$). (Mean value ± standard error. Columns with the same letter are not significantly different ($p > 0.05$).)

The Mg content in the control leaves was 330 ± 60 mg 100 g^{-1}. This value was in accordance with those obtained in other research.[46,47] It should be noted that the contents in these samples were extremely close ($p > 0.05$), which supports the reproducibility of the method adopted here. On the basis of this finding, there was a clear Mg content increase in the leaves after contact with the pectin−$Mg(OH)_2$ nanocomposites. This strongly suggests that the $Mg(OH)_2$ nanoplates were capable of migrating from the pectin edible films.

All samples had significantly higher Mg contents than control ($p < 0.05$) after contact with nanocomposites. The greatest Mg content increase was detected in the sample after 2.5 days contact with the HM pectin−$Mg(OH)_2$ nanocomposite (490 ± 60 mg 100 g^{-1}). Migration from the other nanocomposite films was similar ($p > 0.05$), probably due to the identical $Mg(OH)_2$ concentration present. These results express that the Mg content in arugula leaves was significantly incremented by 45% after contact with the nanocomposites. Accordingly, pectin−$Mg(OH)_2$ nanocomposites show good potential as fortifiers of the magnesium content in foods.

It is important to consider that the increases observed in these assays might have reflected only the migration of $Mg(OH)_2$ nanoplates located at the surface of the nanocomposites. A greater rate of $Mg(OH)_2$ migration could be expected if nanoparticles included in the film bulk are released. In this case, a food matrix with high water activity must be used to increase the diffusivity of polysaccharide film. Future studies will be necessary to assess the influence of these variables, as well as $Mg(OH)_2$ concentration and contact time. Efforts in this subject matter will certainly enable the determination of the full potential of pectin−$Mg(OH)_2$ edible nanocomposites as fortifiers in bioactive packaging.

In conclusion, $Mg(OH)_2$ nanoplates were successfully included in dietary pectin films using the casting/evaporation method. The pectin−$Mg(OH)_2$ nanocomposites exhibited a uniform dispersion of the nanoplates within their matrices, accompanied by strong nanoplate−matrix interactions. In-

clusion of 1 wt % $Mg(OH)_2$ nanoplates substantially increased the tensile properties of the pectin films. Mechanical properties of low-methoxyl pectin rather than high-methoxyl pectin were more affected by the presence of $Mg(OH)_2$ due to the high effectiveness of hydrogen-bonding formation between the nanoplates and the former. Greater quantities of $Mg(OH)_2$ nanoplates (2.5 wt %) improved the thermal stability of the pectin films, and the degree of methoxylation had little influence on these behaviors. Finally, preliminary migration studies confirmed that pectin−$Mg(OH)_2$ nanocomposites are capable of releasing $Mg(OH)_2$ only by contact with foods, thus serving to supplement food products with Mg dosages. This finding allows the exploration of pectin−$Mg(OH)_2$ nanocomposites as new materials for bioactive packaging applications.

■ ASSOCIATED CONTENT

Supporting Information

Surface roughness parameter (R_{rms}) of the pectin−$Mg(OH)_2$ edible nanocomposites (Table S1); additional FTIR spectra for nanocomposite films containing 7 5 wt % $Mg(OH)_2$ and 10 wt % $Mg(OH)_2$ (Figure S1); additional thermal characterization of a LM pectin-based edible film loaded with Mg^{2+} ions (Figure S2); X-ray diffraction characterization of the 5 wt % $Mg(OH)_2$ filled (LM pectin)−$Mg(OH)_2$ nanocomposite treated at different temperatures (Figure S3). This material is available free of charge via the Internet at http://pubs.acs.org.

■ AUTHOR INFORMATION

Corresponding Author

*(L.H.C.M) Postal address: Laboratório Nacional de Nanotecnologia para o Agronegócio, LNNA, Embrapa Instrumentação, CNPDIA, Rua XV de Novembro 1452, 13560-970 São Carlos (SP), Brasil. Phone: +55 (16) 2107-2803. Fax: +55(16) 2107-2902. E-mail: luiz.mattoso@embrapa.br.

Funding

Financial support from Embrapa, FINEP/MCT, CNPq, and CAPES is gratefully acknowledged. F.K.V.M. acknowledges his Ph.D. grant from the FAPESP agency (Project 2010/11584-5). This work is part of the scientific actions promoted by the Rede de Nanotecnologia Aplicada ao Agronegocio (Rede Agronano), Brazil.

Notes

The authors declare no competing financial interest.

■ ACKNOWLEDGMENTS

We thank all of the employees of Embrapa Instrumentation for helpful assistance in this work. We especially thank Prof. Edenir R. P. Filho and his Group of Applied Instrumental Analysis (GAIA) from the Chemistry Department of UFSCar for the FAAS measurements and Dr. Alexandra Manzolli for her cooperation in the AFM studies.

■ REFERENCES

(1) Lopez-Rubio, A.; Gavara, R.; Lagaron, J. M. Bioactive packaging: turning foods into healthier foods through biomaterials. *Trends Food Sci. Technol.* **2006**, *17*, 567−575.

(2) Anderson, J. W.; Baird, P.; Davis, R. H., Jr.; Ferreri, S.; Knudtson, M.; Koraym, A.; Waters, V.; Williams, C. L. Health benefits of dietary fiber. *Nutr. Rev.* **2009**, *67* (4), 188−205.

(3) Lattimer, J. M.; Haub, M. D. Effects of dietary fiber and its components on metabolic health. *Nutrients* **2010**, *2*, 1266−1289.

(4) Maxwell, E. G.; Belshaw, N. J.; Waldron, K. W.; Morris, V. J. Pectin − an emerging new bioactive food polysaccharide. *Trends Food Sci. Technol.* **2012**, *24*, 64−73.

(5) Schols, H. A.; Voragen, A. G. J. The chemical structure of pectins. In *Pectins and Their Manipulation*; Seymour, G. B., Knox, J. P., Eds.; Blackwell Publishing and CRC Press: Oxford, UK, 2002; pp 1−29.

(6) Willats, W. G. Y.; Knox, J. P.; Mikkelsen, J. D. Pectin: new insights into an old polymer are starting to gel. *Trends Food Sci. Technol.* **2006**, *17*, 97−104.

(7) Gorrasi, G.; Bugatti, V.; Vittoria, V. Pectins filled with LDH-antimicrobial molecules: preparation, characterization and physical properties. *Carbohydr. Polym.* **2012**, *89*, 132−137.

(8) Vartiainen, J.; Tammelin, T.; Pere, J.; Tapper, U.; Harlin, A. Biohybrid barrier films from fluidized pectin and nanoclay. *Carbohydr. Polym.* **2010**, *82*, 989−996.

(9) Cavallaro, G.; Lazzara, G.; Milioto, S. Dispersions of nanoclays of different shapes into aqueous and solid biopolymeric matrices. Extended physicochemical study. *Langmuir* **2011**, *27* (3), 1158−1167.

(10) De Moura, M. R.; Avena-Bustillos, R. J.; McHugh, T. H.; Krochta, J.; Mattoso, L. H. C. Improved barrier and mechanical properties of novel hydroxypropyl methylcellulose edible films with chitosan/tripolyphosphate nanoparticles. *J. Food Eng.* **2009**, *92*, 448−453.

(11) De Moura, M. R.; Lorevice, M. V.; Mattoso, L. H. C.; Zucolotto, V. Highly stable, edible cellulose films incorporating chitosan nanoparticles. *J. Food Sci.* **2011**, *76* (2), 27−29.

(12) Lorevice, M. V.; De Moura, M. R.; Aouada, F. A.; Mattoso, L. H. C. Development of novel guava puree films containing chitosan nanoparticles. *J. Nanosci. Nanotechnol.* **2012**, *12*, 2711−2717.

(13) Azeredo, H. M. C.; Mattoso, L. H. C.; Wood, D.; Willams, T. G.; Avena-Bustillos, R.; McHugh, T. H. Nanocomposite edible films from mango puree reinforced with cellulose nanofibers. *J. Food Sci.* **2009**, *74* (5), 31−35.

(14) Azeredo, H. M. C.; Mattoso, L. H. C.; Avena-Bustillos, R.; Filho, G. C.; Wood, D.; Munford, M. L.; McHugh, T. H. Nanocellulose reinforced chitosan composite films as affected by nanofiller loading and plasticizer content. *J. Food Sci.* **2010**, *75* (1), 1−7.

(15) Peng, X.; Ren, J.; Zhong, L.; Sun, R. Nanocomposite films based on xylan-rich hemicelluloses and cellulose nanofibers with enhanced mechanical properties. *Biomacromolecules* **2011**, *12*, 3321−3329.

(16) Janjarasskul, T.; Krochta, J. M. Edible packaging materials. *Annu. Rev. Food Sci. Technol.* **2010**, *1*, 415−448.

(17) Carrado, K. A. Introduction: Clay structure, surface acidity, and catalysis. *Handbook of Layered Materials*; Auerbach, S. M., Carrado, K. A., Dutta, P. K., Eds.; Dekker: New York, 2004; pp 1−39.

(18) Frost, R. L.; Kloprogge, J. T. Infrared emission spectroscopic study of brucite. *Spectrochim. Acta, Part A* **1999**, *55*, 2195−2205.

(19) Sun, X.; Xiang, L. Hydrothermal conversion of magnesium oxysulfate whiskers to magnesium hydroxide nanobelts. *Mater. Chem. Phys.* **2008**, *109*, 381−385.

(20) Hornsby, P. R.; Watson, C. L. A study of the mechanism of flame retardancy and smoke suppression in polymers filled with magnesium hydroxide. *Polym. Degrad. Stab.* **1990**, *30*, 73−87.

(21) Rothon, R. N.; Hornsby, P. R. Flame retardant effects of magnesium hydroxide. *Polym. Degrad. Stab.* **1996**, *54*, 383−385.

(22) Liu, H.; Wang, R.; Xu, X. Thermal stability and flame retardancy of PET/magnesium salt composites. *Polym. Degrad. Stab.* **2010**, *95*, 1466−1470.

(23) Zheng, X.-T.; Wu, D.-M.; Meng, Q.-Y.; Wang, K.-J.; Liu, Y.; Wan, L.; Ren, D.-Y. Mechanical properties of low-density polyethylene/nano-magnesium hydroxide composites prepared by an in situ bubble stretching method. *J. Polym. Res.* **2008**, *15*, 59−65.

(24) Moreira, F. K. V.; Pedro, D. C.A.; Glenn, G. M.; Marconcini, J. M.; Mattoso, L. H. C. Brucite nanoplates reinforced starch bionanocomposites. *Carbohydr. Polym.* **2013**, *92*, 1743−1751.

(25) Hwang, C.; Ross, V.; Mahadevan, U. Micronutrient deficiencies in inflammatory bowel disease: from A to zinc. *Inflamm. Bowel Dis.* **2012**, *18* (10), 1961−1981.

(26) Geiger, H.; Wanner, C. Magnesium in disease. *Clin. Kidney J.* **2012**, *5* (1), 25−38.
(27) Nielsen, F. H. Magnesium, inflammation, and obesity in chronic disease. *Nutr. Rev.* **2010**, *68* (6), 333−340.
(28) Rosanoff, A.; Weaver, C. M.; Rude, R. K. Suboptimal magnesium status in the United States: are the health consequences underestimated? *Nutr. Rev.* **2012**, *70* (3), 153−164.
(29) Weglicki, W. B. Hypomagnesemia and inflammation: clinical and basic aspects. *Annu. Rev. Nutr.* **2012**, *32*, 55−71.
(30) ASTM D882-09. Standard test method for tensile properties of thin plastic sheeting. In *Annual Book of American Standard Testing Methods*; ASTM: Philadelphia, PA, 2009.
(31) Avella, M.; Vlieger, J. J.; Errico, M. E.; Fischer, S.; Vacca, P.; Volpe, M. G. Biodegradable starch/clay nanocomposite films for food packaging applications. *Food Chem.* **2005**, *93*, 467−474.
(32) Baranek, Ph.; Lichanot, A.; Orlando, R.; Dovesi, R. Structural and vibrational properties of solid $Mg(OH)_2$ and $Ca(OH)_2$ − performance of various Hamiltonians. *Chem. Phys. Lett.* **2001**, *340*, 362−369.
(33) Fenoglio, I.; Fubini, B.; Ghibaudi, E. M.; Turci, F. Multiple aspects of the interaction of biomacromolecules with inorganic surfaces. *Adv. Drug Delivery Rev.* **2011**, *63*, 1186−1209.
(34) Riddick, T. M. *Control of Colloid Stability through Zeta Potential*; Zeta-Meter Inc. via Livingston Publishing: Wynnewood, PA, 1968.
(35) Iwanaga, D.; Gray, D.; Decker, E. A.; Weiss, J.; McClements, D. J. Stabilization of soybean oil bodies using protective pectin coatings formed by electrostatic deposition. *J. Agric. Food Chem.* **2008**, *56*, 2240−2245.
(36) Lutz, R.; Aserin, A.; Wicker, L.; Garti, N. Structure and physical properties of pectins with block-wise distribution of carboxylic acid groups. *Food Hydrocolloids* **2009**, *23*, 786−794.
(37) Bengoechea, C.; Jones, O. G.; Guerrero, A.; McClements, D. J. Formation and characterization of lactoferrin/pectin electrostatic complexes: Impact of composition, pH and thermal treatment. *Food Hydrocolloids* **2011**, *25*, 1227−1232.
(38) McLaughlin, W. J.; White, J. L.; Hem, S. L. The surface chemistry of agglomerates formed in suspensions containing aluminum hydroxycarbonate and magnesium hydroxide. *J. Colloid Interface Sci.* **1993**, *158*, 333−341.
(39) Kaboorani, A.; Riedl, B.; Blanchet, P.; Fellin, M.; Hosseinaei, O.; Wang, S. Nanocrystalline cellulose (NCC): a renewable nano-material for polyvinyl acetate (PVA) adhesive. *Eur. Polym. J.* **2012**, *48*, 1829−1837.
(40) Synytsya, A.; Čopíková, J.; Matějkab, P.; Machovič, V. Fourier transform Raman and infrared spectroscopy of pectins. *Carbohydr. Polym.* **2003**, *54*, 97−106.
(41) Braterman, P. S.; Cygan, R. T. Vibrational spectroscopy of brucite: a molecular simulation investigation. *Am. Mineral.* **2006**, *91*, 1188−1196.
(42) Darder, M.; López-Blanco, M.; Aranda, P.; Aznar, A. J.; Bravo, J.; Ruiz-Hitzky, E. Microfibrous chitosan-sepiolite nanocomposites. *Chem. Mater.* **2006**, *18*, 1602−1610.
(43) Moreira, F. K. V.; Marconcini, J. M.; Mattoso, L. H. C. Analysis of the influence of composition and processing parameters on the mechanical properties of biodegradable starch/pectin blends. *Polym. Bull.* **2012**, *69*, 561−577.
(44) Paul, D. R.; Robeson, L. M. Polymer nanotechnology: nanocomposites. *Polymer* **2008**, *49*, 3187−3183.
(45) Ray, S. S.; Bousmina, M. Biodegradable polymers and their layered silicate nanocomposites: In greening the 21st century materials world. *Prog. Mater. Sci.* **2005**, *50*, 962−1079.
(46) Barlas, N. T.; Irget, M. E.; Tepecik, M. Mineral content of the rocket plant (*Eruca sativa*). *Afr. J. Biotechnol.* **2011**, *64*, 14080−14082.
(47) Bozokalfa, M. K.; Eşiyok, D.; Yağmur, B. Use of multivariate analysis in mineral accumulation of rocket (*Eruca sativa*) accessions. *Genetika* **2011**, *43*, 437−448.